



3 4456 0381134 7

ORNL/TM-12718

ornl

**OAK RIDGE
NATIONAL
LABORATORY**

MARTIN MARIETTA

Cadmium Verification Measurements of HFIR Shroud Assembly 22

Jeffrey A. Chapman
Frederick J. Schultz

OAK RIDGE NATIONAL LABORATORY

CENTRAL RESEARCH LIBRARY

CIRCULATION SECTION

4300N ROOM 125

LIBRARY LOAN COPY

DO NOT TRANSFER TO ANOTHER PERSON

If you wish someone else to see this
report, send in name with report and
the library will arrange a loan.

NON-7589-01875

MANAGED BY
MARTIN MARIETTA ENERGY SYSTEMS, INC.
FOR THE UNITED STATES
DEPARTMENT OF ENERGY

ORNL/TM-12718

506
201

Waste Management and Remedial Action Division
Applied Radiation Measurements Department

**Cadmium Verification Measurements of
HFIR Shroud Assembly 22**

Jeffrey A. Chapman
Frederick J. Schultz

Date Published---April 1994

Prepared by the
OAK RIDGE NATIONAL LABORATORY
Oak Ridge, Tennessee 37830
Managed by MARTIN MARIETTA ENERGY SYSTEMS, INC.
for the
U.S. DEPARTMENT OF ENERGY
under contract DE-AC05-84OR21400



3 4456 0381134 7

ABSTRACT

Radiation-based nondestructive examination methods have been used to successfully verify the presence of cadmium in High Flux Isotope Reactor (HFIR) spent-fuel shroud assembly number 22 (SA22). These measurements show, in part, that SA22 is certified to meet the criticality safety specifications for a proposed reconfiguration of the HFIR spent-fuel storage array. [2] Measurement of the unique 558.6-keV gamma-ray from neutron radiative capture on cadmium provided conclusive evidence for the presence of cadmium in the outer shroud of the assembly. Cadmium verification in the center post and outer shroud was performed by measuring the degree of neutron transmission in SA22 relative to two calibration shroud assemblies. Each measurement was performed at a single location on the center post and outer shroud. These measurements do not provide information on the spatial distribution or uniformity of cadmium within an assembly. Separate measurements using analog and digital radiography were performed to a) globally map the continuity of cadmium internal mass, and b) locally determine the thickness of cadmium. Radiography results will be reported elsewhere. The measurements reported here should not be used to infer the thickness of cadmium in either the center post or outer shroud of an assembly.

Measurement criteria for establishing the presence of cadmium were satisfied. Measurement results of SA22 compare very well with those of SA70, a calibration assembly containing cadmium. Results of calibration assembly SA00 (no cadmium) were significantly different from either SA22 or SA70. In SA22 and SA70, the 558.6-keV capture gamma-ray was clearly observed; in SA00 it was not. In SA22, two less intense gamma-rays from cadmium were also observed at 651.3- and 1364.3-keV, providing additional evidence for the presence of cadmium. In the shrouds of SA22 and SA70, neutron absorption was a factor of 8-10 greater than in SA00. In the posts of SA22 and SA70, neutron absorption was a factor of 5-6 greater than in SA00.

The theory, methodology, instrumentation, and analysis methods are presented in reference 3 along with the measurement results for SA70 and SA00, the calibration assemblies. Results presented herein along with the control charts that compare SA22 measurements with those from the calibration assemblies show conclusive evidence of cadmium in SA22.

We gratefully acknowledge the assistance provided by the HFIR engineering staff: Dowe Dabbs, Victor Cain, John Kieth, and Mike Waters; and the Waste Examination and Assay Facility staff: Larry Pierce, Richard Bailey, David Hensley, and Phillip Womble. Larry Pierce was instrumental in preparing the AutoCad™ drawings and in machining and assembling the source holders, moderators, and collimators. Richard Bailey was primarily responsible for coordinating radiography measurements.

TABLE OF CONTENTS

Abstract	<i>i</i>
1.0 Summary	1
2.0 Results	5
2.1 Gamma-ray Spectroscopy	5
2.1.1 Radiative Neutron Capture on Cadmium	5
2.1.2 Contaminants	11
2.2 Neutron Transmission	13
2.2.1 Post	13
2.2.2 Shroud	14
3.0 Conclusions	15
4.0 References	17
App. A. Gamma-ray Region-of-Interest Output for SA22	18
A.1 Shroud Gamma-ray Background Spectrum	18
A.2 Shroud Gamma-ray Spectrum with ²⁵² Cf Source	20
A.3 Stripped Gamma-ray Spectrum	22
App. B. Neutron Region-of-Interest Output for SA22	23
App. C. Analysis Worksheet	26

LIST OF TABLES

Table 1.1.	Summary of Measurement Results	3
Table 2.1.	Cadmium Verification Photopeaks from Neutron Capture	8

LIST OF FIGURES

Figure 1.1.	Measured Neutron Flux Corrected for $1/r^2$ Geometry Effect Between Post and Shroud Configurations (cps)	4
Figure 2.1.	Gamma-ray Spectrum of SA22 with Background Superimposed (In Region of 558.6-keV Cd-capture gamma-ray)	6
Figure 2.2.	Stripped Gamma-ray Spectrum of SA22 with Original Background Spectrum Superimposed	7
Figure 2.3.	Integrated Peak Area for Stripped Gamma-ray Spectrum of SA22 In Region of 558.6-keV Cd-capture Gamma-ray	7
Figure 2.4.	Composite Gamma-ray Spectrum for SA22	9
Figure 2.5	Intercomparison of SA22, SA70, and SA00 in 558.6-keV Region	10
Figure 2.6.	Relative Measured Activity of Detected Isotopes	11
Figure 2.7.	SA22 Post Neutron Background (ROI1)	13
Figure 2.8.	SA22 Post Neutron Measurement (ROI1)	13
Figure 2.9.	SA22 Shroud Neutron Background (ROI1)	14
Figure 2.10	SA22 Shroud Neutron Measurement (ROI1)	14
Figure 3.1	Control Chart of 558.6-keV Gamma-ray Ratios---Test Assemblies to SA70	15
Figure 3.2.	Control Chart of Neutron Flux Ratios---Test Assemblies to Calibration Assemblies (Post)	16
Figure 3.3.	Control Chart of Neutron Flux Ratios---Test Assemblies to Calibration Assemblies (Shroud)	16

1.0 SUMMARY

Gamma-ray spectroscopy and neutron transmission measurements have conclusively verified the presence of cadmium in the center post and outer shroud of HFIR shroud assembly number 22 (SA22), reported to contain a nominal cadmium thickness of 58 mil in the center post and 36 mil in the outer shroud. Measurements of SA22 were normalized and compared to reference measurements performed on calibration shroud assemblies SA00 and SA70. SA00 does not contain cadmium; SA70 contains 36-mil thick cadmium in both the post and the shroud. Reference calibration measurements, methodology, experimental setup, and data analysis and interpretation are reported in ORNL/TM-12627, "*Verification of Cadmium in HFIR Spent Fuel Shroud Assemblies by Neutron Induced Gamma-Ray Spectroscopy and Neutron Transmission Measurements.*" [3] Verification measurements for SA22 were performed according to the principles described in ORNL/TM-12627 and in HFIR work package 31674, part 22B.

A single-point gamma-ray spectroscopy measurement of gamma-rays created from radiative neutron capture in cadmium was performed. Physical size restrictions limited these measurements to the outer shroud of the assembly; the post and base of the assembly were not measured. Detector acquisition times were selected to achieve a statistical counting error of less than 5 percent for the 558.6-keV prompt gamma-ray from cadmium. Reference gamma-ray spectra of calibration assemblies SA00 and SA70 were acquired for 20 minutes, each. Spectra of SA22 were acquired for 2 hours because of interfering photopeaks and dead time losses from the presence of ^{152}Eu , ^{154}Eu , ^{137}Cs , and ^{60}Co contaminants. The gamma-ray spectrum from radiative neutron capture was corrected for background gamma-ray interferences by directly measuring and subtracting the background spectrum, channel-by-channel. A ^{252}Cf source emitting $10,000 \text{ n s}^{-1}$ over $4\text{-}\pi$ steradian was used to produce a flux of interrogating neutrons for the neutron-capture reactions. Polyethylene was used to moderate source neutrons closer to energies required to induce the capture reactions. A lead collimator interposed between the assembly and the gamma-ray detector provided shielding from extraneous gamma-rays, primarily from intrinsic activation and fission product contamination on the assembly. Gamma-ray measurements were acquired using a high-resolution, high-purity, solid-state, germanium detector coupled to an electronics package that allows analog to digital conversion of pulses and subsequent display and analysis on a multi-channel analyzer.

Four, single-point neutron transmission measurements were performed on SA22: a neutron source and background measurement on the center post and outer shroud, each. Detector acquisition times were selected to achieve a statistical counting error of less than 5 percent. Posts were measured for 10 minutes, shrouds for 10 minutes. A PuF_4 (α, n) source was used to produce a flux of transmission neutrons, about $150,000 \text{ n s}^{-1}$ over $4\text{-}\pi$ steradian. Polyethylene was used to moderate source neutrons closer to thermal energies. Neutron flux measurements were made with a pressurized (4-atmosphere), ^3He proportional detector, 1-in diameter by 6-in in length. The detector was coupled to an electronics package that allows analog to digital conversion of pulses and subsequent display and analysis on a multi-channel analyzer.

Measurement criteria for establishing the presence of cadmium in an assembly were essentially two-fold: (1) observe the unique gamma-ray signature from cadmium in SA22 (test assembly) and SA70 (calibration assembly with cadmium), but not in SA00 (calibration assembly without cadmium). The ratio of the 558.6-keV gamma-ray yields of SA22 and SA70 should be near unity; and (2) observe a significant reduction in transmitted thermal neutron flux through SA22 and SA70 relative to the transmitted flux through SA00. These measurement criteria were satisfied for SA22. Measurement criteria did not include estimating cadmium thickness. This criteria was measured via a separate technique. [12]

As indicated by the summary of results presented in Table 1.1, the measurements performed on SA70 and SA22 compare to within 1% for gamma-ray measurements and to within 15% for neutron transmission measurements. Both gamma-ray and neutron measurements for SA70 and SA22 were significantly different from the measurements conducted on SA00. As expected for SA00, no characteristic gamma-ray from cadmium was detected and a factor of 10 more neutrons was transmitted through the shroud. Table 1.1 shows for each assembly the net measured gamma-ray and neutron count rate and the associated standard deviation (1s). A brief intercomparison of shroud-to-post neutron flux ratios is also presented, but uncorrected for measurement geometry.

Table 1.1 Summary of Measurement Results

Measurement	Measured count rate \pm s (sec ⁻¹)			Normalized Results	
	SA22	SA70	SA00	SA22/SA70	SA00/SA22
Radiative n-capture					
558.6 keV gamma-ray	1.84	1.78	ND	1.03	0
n-transmission					
Φ_n , center post *	3.59 \pm 0.08	3.77 \pm 0.08	22.09 \pm 0.19	0.95 \pm 0.03	6.16 \pm 0.16
Φ_n , outer shroud **	11.66 \pm 0.22	13.83 \pm 0.24	113.19 \pm 0.69	0.84 \pm 0.02	9.71 \pm 0.21
Φ_n ratios *** shroud to post	3.25 \pm 0.09	3.67 \pm 0.10	5.13 \pm 0.05		
Nominal Cd thickness					
Post (mil) *	116	72	0		
Shroud (mil) **	36	36	0		

* Post: measurement through 2 layers of cadmium, 58-mil, each (SA22), 36-mil, each (SA70), source to detector distance = 10in.

** Shroud: measurement through 1 layer of cadmium, 36-mil (SA22), 36-mil (SA70), source to detector distance = 6in.

*** Not corrected for counting geometry

Φ_n : Thermal neutron flux, s: standard deviation, ND: Not Detected

Cadmium capture gamma-ray measurements met the verification criteria:

- (1) both SA22 and SA70 showed a production rate of 558.6-keV gamma-rays equal to about 1.8 counts per second, corresponding to about 4000 gamma-rays per second per steradian. Because SA22 was counted for a much longer period of time, two additional gamma-rays were detected from cadmium neutron capture: 651.3- and 1634.3-keV; and
- (2) No prompt 558.6-keV gamma-rays were observed for measurements conducted on SA00. [3]

Neutron transmission measurements also met the measurement criteria:

- (1) the center posts of SA22 and SA70 were opaque to thermal neutrons by a factor of 5 to 6 over SA00, a significant difference;

- (2) the outer shrouds of SA22 and SA70 were opaque to thermal neutrons by a factor of 8 to 10 over SA00, a significant difference; and
- (3) SA22 results were very consistent with those of SA70. Thermal neutron flux ratios for SA22/SA70 were 0.95 (post) and 0.84 (shroud).

Neutron measurement results should not be used to make a judgement about cadmium thickness. The results incorrectly indicate that the shrouds are more absorbing than the posts (10 versus 6), in spite of the fact that there is actually more cadmium in the posts. Because the bare ^3He detector was not shielded to prevent measuring thermal neutrons from all directions, the scattered component of the flux could not be separated from the more "direct" component. The ^3He counter measures a greater fraction of the scattered flux in the post geometry than it does in the shroud geometry, particularly in the presence of cadmium. As a result, the change in measured flux between the post and the shroud is different depending on whether cadmium is present or not. This is illustrated in Figure 1.1, showing that an accurate measure of cadmium thickness is not plausible when the measurements are referenced to SA00, the calibration assembly without cadmium. Variations in neutron background, counting statistics, and slight differences between counting configurations also affect these results, although to a lesser degree.

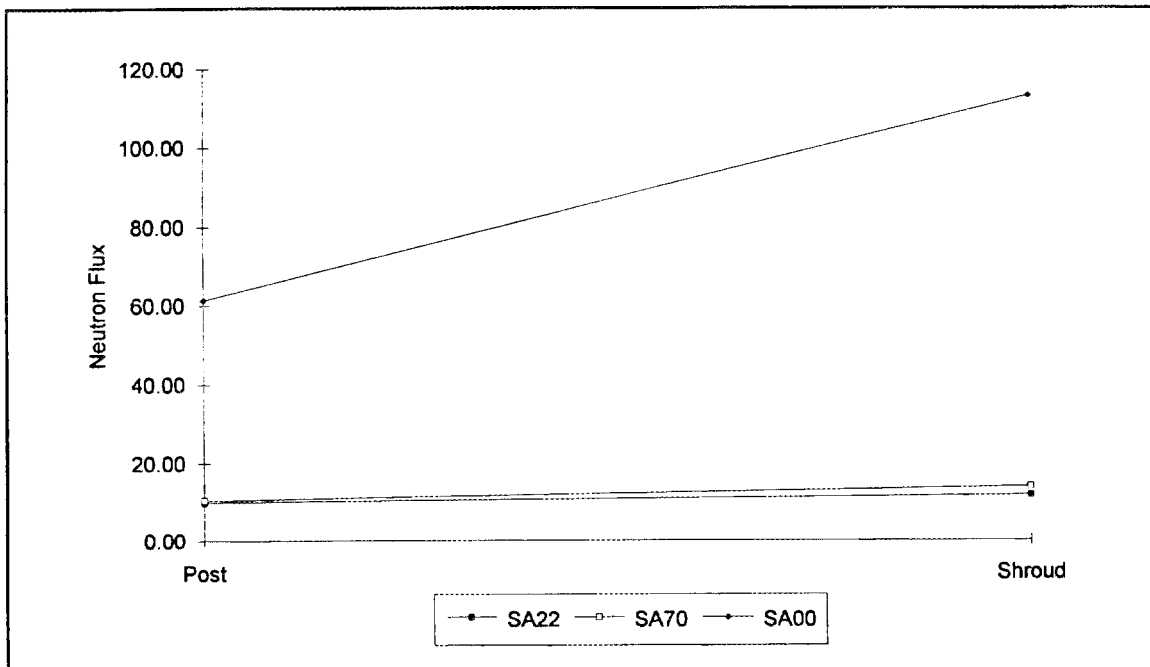


Figure 1.1. Measured Neutron Flux Corrected for $1/r^2$ Geometry Effect Between Post and Shroud Configurations (cps)

2.0 RESULTS

Measurement results are presented in the following two subsections. First, the gamma-ray spectra are presented showing the primary 558.6-keV gamma-ray signature from cadmium neutron capture. Secondary and tertiary gamma-rays from cadmium were also measured, one at 651.3 keV, the other at 1364.3 keV. Second, neutron transmission pulse-height distributions are presented to demonstrate the effective reduction in thermal neutron flux when cadmium is present in the assembly.

The gamma-ray and neutron transmission measurements were made at the same location on the shroud---about 10 to 12 inches from the top lip. Neutron transmission measurements on the post were also made at one location, about 10 to 12 inches from the top lip. The shroud measurement location was determined on the basis of a radiation survey to locate the spot where the external radiation exposure rate was at a minimum, in this case about 2 mR h⁻¹ on contact. External radiation rates were caused by activation and fission product contaminants on and within the shroud assembly. The reason for finding the location with the smallest contact radiation survey reading was to minimize acquisition dead-time and reduce gamma-ray interferences.

2.1 Gamma-ray Spectroscopy

Two spectra were acquired: a background and a source spectrum. First, a background spectrum was acquired in the shroud counting geometry. Second, a spectrum was acquired in the same counting geometry with the ²⁵²Cf source in place. [3] Photopeak data from the acquired gamma-ray spectra was reduced according to reference 3 using analysis tools available with APTEC™ software version 4.3.[11] The following sequence was performed to determine the integral number of detected gamma-ray events at the cadmium energy of 558.6 keV in the presence of a smaller ¹⁵⁴Eu gamma-ray at 557.6 keV: the energy-offset of the background spectrum was normalized to that of the source spectrum prior to subtraction of the background spectrum; a 3-point smooth was performed on the net spectrum to average out local perturbations that result from a channel-by-channel subtraction; and peak search parameters were: straight line background subtraction beneath the photopeak, centroid was calculated between gross half maximum, centroid weighting was applied as the net counts times the channel, and most importantly, the statistical error of the photopeak must be less than 5% to be considered an actual peak.

2.1.1 Radiative Neutron Capture on Cadmium

Figure 2.1 shows uncorrected data of the gamma-ray pulse-height spectrum with the ^{252}Cf source irradiating the shroud; background is superimposed beneath the source spectrum. Notice, in particular, the interfering ^{154}Eu gamma ray at 557.6 keV; however, the 558.6-keV photopeak from cadmium is noticeably larger than the contribution from ^{154}Eu . Neighboring photopeaks include: 511 keV (annihilation), 564 keV (^{152}Eu), 582 keV (^{154}Eu), 586.3 keV (^{152}Eu), and 591.8 keV (^{154}Eu). The source spectrum is slightly more intense than the background spectrum, about a difference of 2000 counts in the Compton continuum in the neighboring region of the 558.6-keV prompt gamma-ray. The small 557.6 keV photopeak from ^{154}Eu is noticeable in the background spectrum while, in the source spectrum, the 558.6-keV photopeak from Cd is broadened from its contribution. Figure 2.1 illustrates why it is important that the ^{154}Eu background photopeak be accounted for when reporting the net signal from cadmium capture.

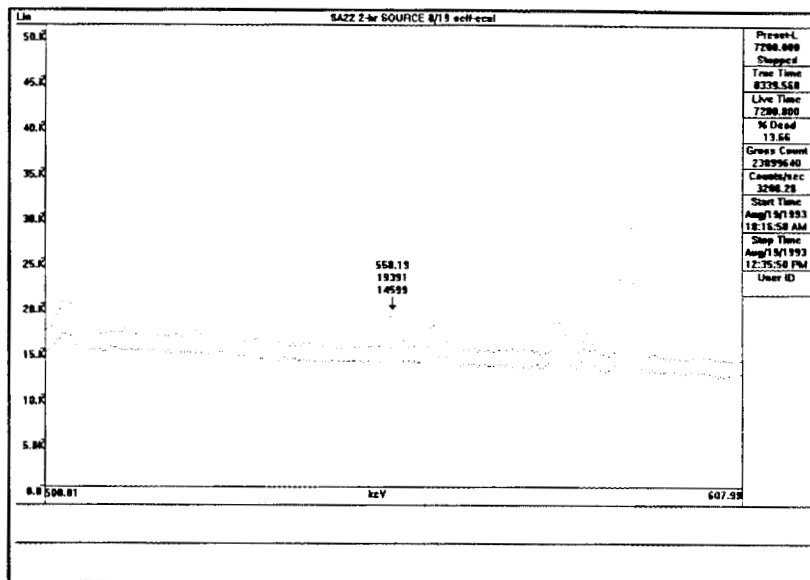


Figure 2.1. Gamma-ray Spectrum of SA22 with Background Superimposed (In Region of 558.6-keV Cd-capture gamma-ray)

Figure 2.2 shows the spectrum from 500 keV up to about 1600 keV. The net "stripped" spectrum is shown in addition to the original background spectrum. Stripping, used in this context, means to subtract the background spectrum from the source spectrum channel-by-channel. To assure an accurate representation of the stripped "net" photopeak, the spectra were corrected for shifts in the detector amplifier gain. Both spectra were calibrated for energy using the known energies emitted by the contaminants ^{152}Eu , ^{154}Eu , ^{137}Cs , and ^{60}Co ; normalized for live time. Peak identification was referenced against the gamma-ray library D:\HFIR_CD\HFIR.LIB (Appendix E of reference 3). The background spectrum was then shifted downward by the linear difference in 6.4 and 5.55, since the zero-offset for the background was 6.4 while that of the source spectrum was 5.55 (see Appendices A.1 and

A.2). As seen in the Appendix A printouts, there was no appreciable difference in the gain between the two spectra (0.3930 keV chan⁻¹ vs. 0.3923 keV chan⁻¹).

Measurement dead-time was reduced to less than 13% by using a lead collimator between the shroud and the detector and by increasing the Analog-to-Digital Converter (ADC) lower level discriminator to a setting equivalent to about 500 keV, thus reducing the contributions to the count rate processed by the multi-channel analyzer.

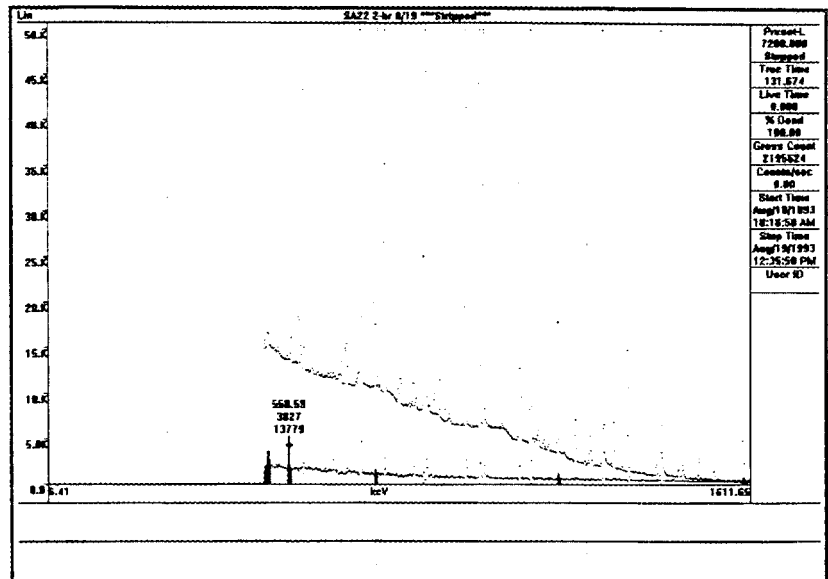


Figure 2.2. Stripped Gamma-ray Spectrum of SA22 with Original Background Spectrum Superimposed

Figure 2.3 is an expanded view of the 558.6-keV region of the net stripped spectrum. The resulting photopeak is slightly broadened (FWHM-2.23 keV), but yields significant evidence for the presence of cadmium despite the contribution from ¹⁵⁴Eu. From the data presented in Appendix A.3, the 558.6-keV peak was identified as region-of-interest (ROI) 3, 13223 ± 115 net counts for a 7200-sec acquisition time. The fitted peak centroid was 558.47 keV with a FWHM of 2.23 keV---the peak was broadened, but adequately accounted for, from the contribution of the Eu contamination.

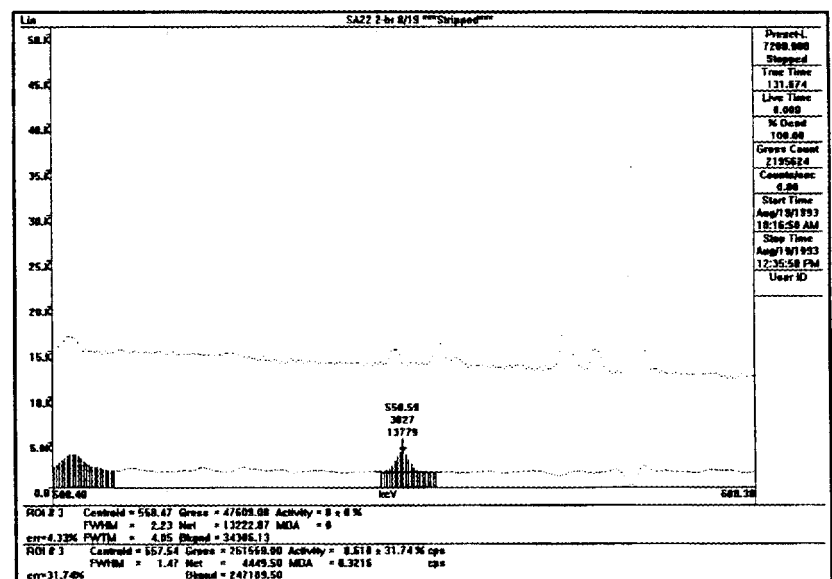


Figure 2.3. Integrated Peak Area for Stripped Gamma-ray Spectrum of SA22 In Region of 558.6-keV Cd-capture Gamma-ray

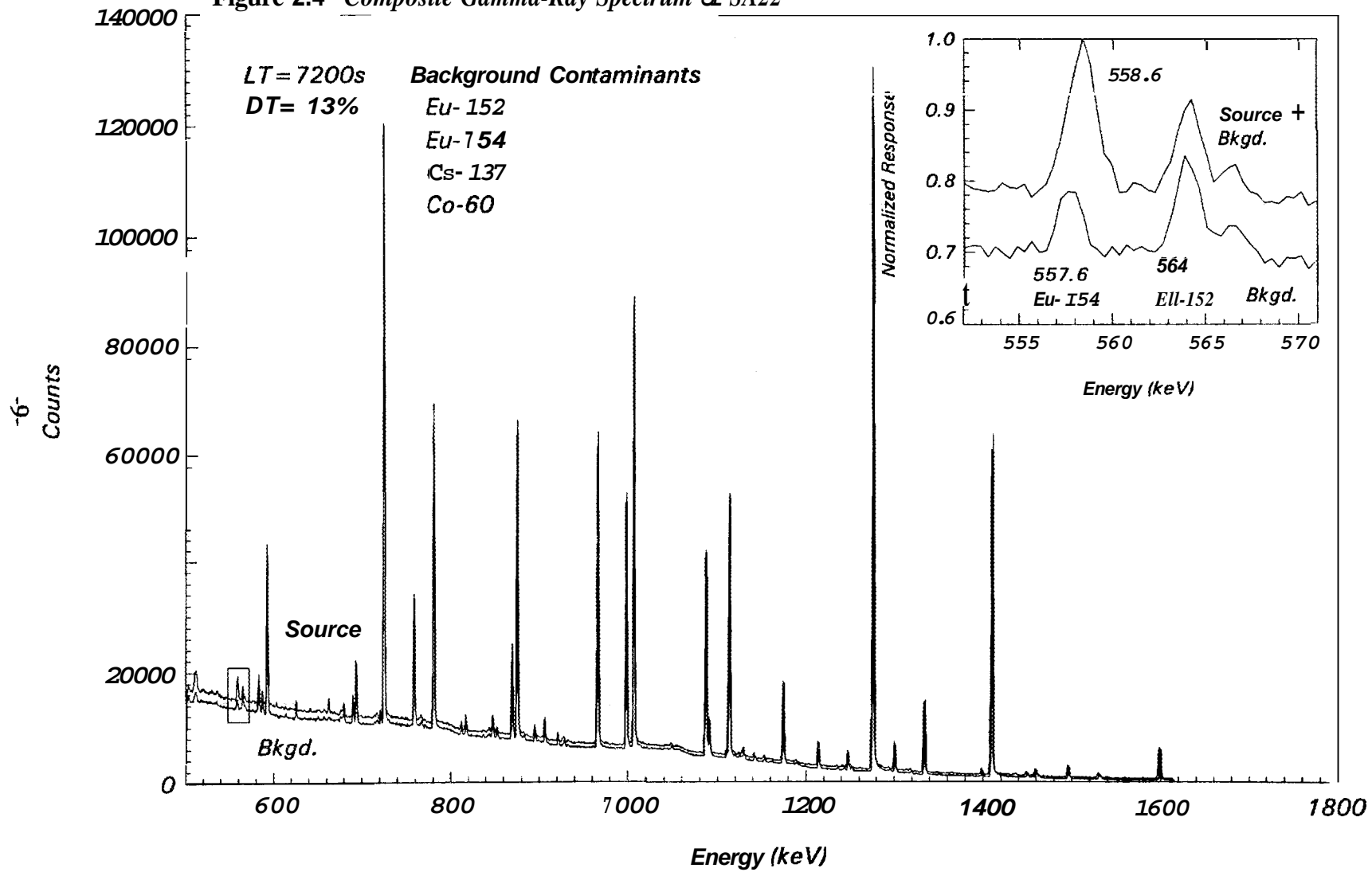
Figure 2.4 is the complete, as-measured neutron-induced gamma-ray spectrum of SA22 with the background spectrum superimposed. The large photopeaks are from the contaminants. The expanded window within the figure shows the difference between the background spectrum and the source spectrum in the region of the 558.6-keV gamma-ray. Appendix A contains copies of the peak-fitting output from the background, source, and net spectral data files. For a 2-hour counting period, two additional gamma-ray photopeaks from cadmium neutron capture were observed: 651.3- and 1364.3-keV. Photopeak results for SA22 are presented in Table 2.1. The normalized count rate was obtained by dividing the measured count rate by the corresponding gamma-ray yield per neutron capture. No correction was made for absolute detector efficiency because of the difficult counting geometry. In comparison, SA70---the calibration assembly, the integral number of events under the 558.6-keV photopeak was 2137 ± 46 net counts for a 1200-sec acquisition time. The fitted-peak centroid was 558.25 keV with a FWHM of 1.5 keV.[3]

Table 2.1. Cadmium Verification Photopeaks from Neutron Capture

Energy (keV)	counts per sec (cps)	Yield per capture	Normalized cps
558.6	1.8 ± 0.015	0.72	2.53 ± 0.021
651.3	0.61 ± 0.0092	0.14	4.41 ± 0.066
1364.3	0.24 ± 0.0058	0.05	4.85 ± 0.117

Figure 2.5 shows from top to bottom an intercomparison of the 558.6-keV gamma-ray regions for SA22(test), SA70(Cd), and SA00(No Cd). The pulse-height distributions were normalized by the number of counts in the channel closest to 558.6-keV. In contrast to SA22, SA70 contains a minimal background and does not include the interference from ^{154}Eu . Only compton background radiation was observed in SA00.

Figure 2.4 Composite Gamma-Ray Spectrum of SA22



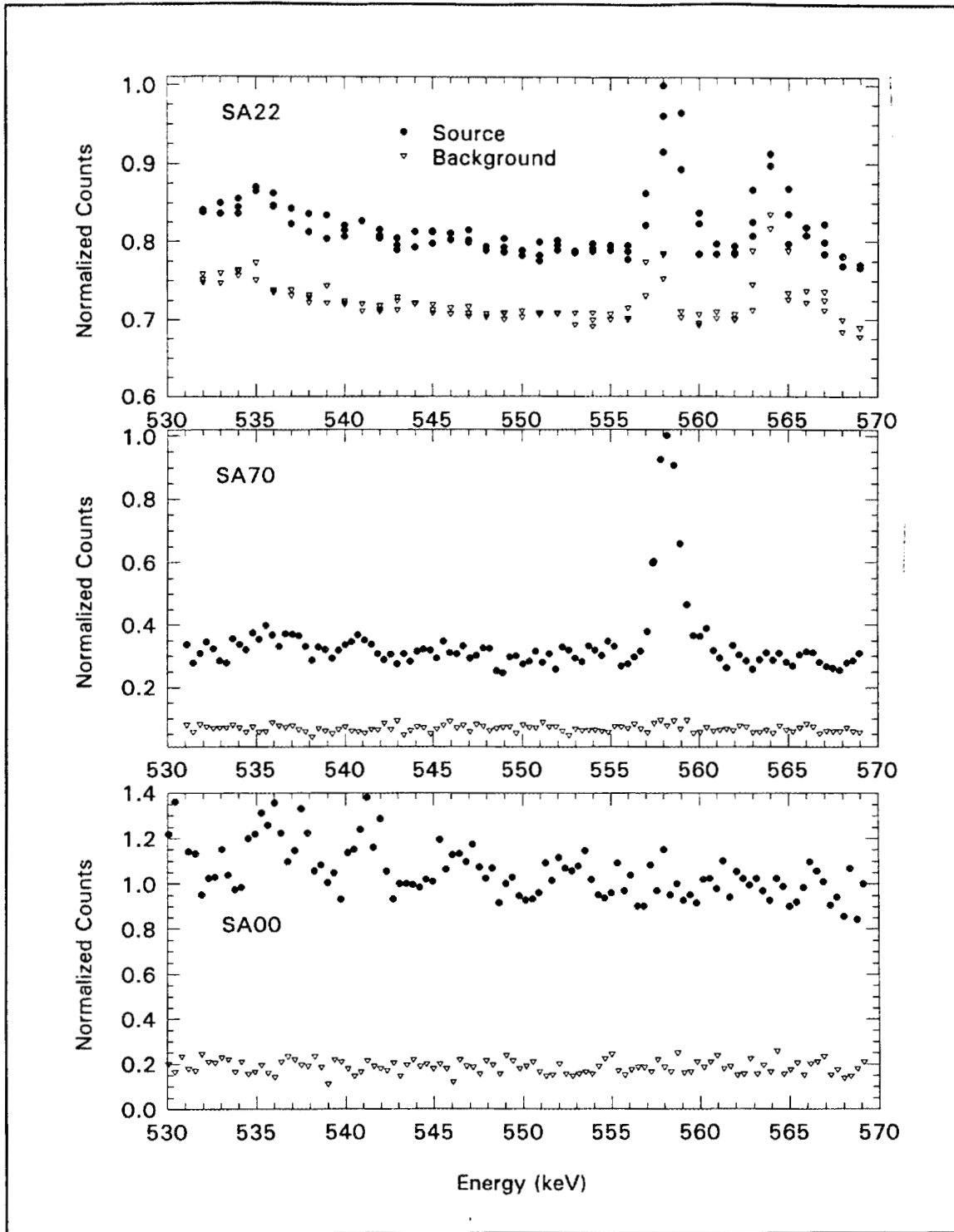


Figure 2.5 *Intercomparison of SA22, SA70, and SA00 in 558.6-keV Region*
 Unlike SA70, SA22 at the top shows the background contribution and interference from ^{154}Eu . SA00 is random background.

2.1.2 Contaminants

As mentioned earlier, gamma emitting contaminants were measured in SA22. The measurement results are presented here to establish a comparison of data between the population of test assemblies and to show the relative magnitude of possible interferences from the contaminants. As shown in Figure 2.6, the relative gamma-ray efficiency of the HPGe detector is easily constructed by plotting the yield-corrected photopeak counts of the contaminant isotopes: ^{152}Eu , ^{154}Eu , ^{60}Co , and ^{137}Cs . This calculated intrinsic detector efficiency calibration provides relative activities of the contaminant isotopes. It does not provide absolute quantities because the true radioactivities of the contaminants are not known. Subsequently, a statement about the nature of the contaminants within the assembly is that the Eu isotopes are nearly equivalent in activity, ^{60}Co is $1/20^{\text{th}}$ that of Eu, and ^{137}Cs is $1/350^{\text{th}}$ that of Eu. Unlike an efficiency function for a point source, the efficiency function here has a very small slope, as expected.[3]

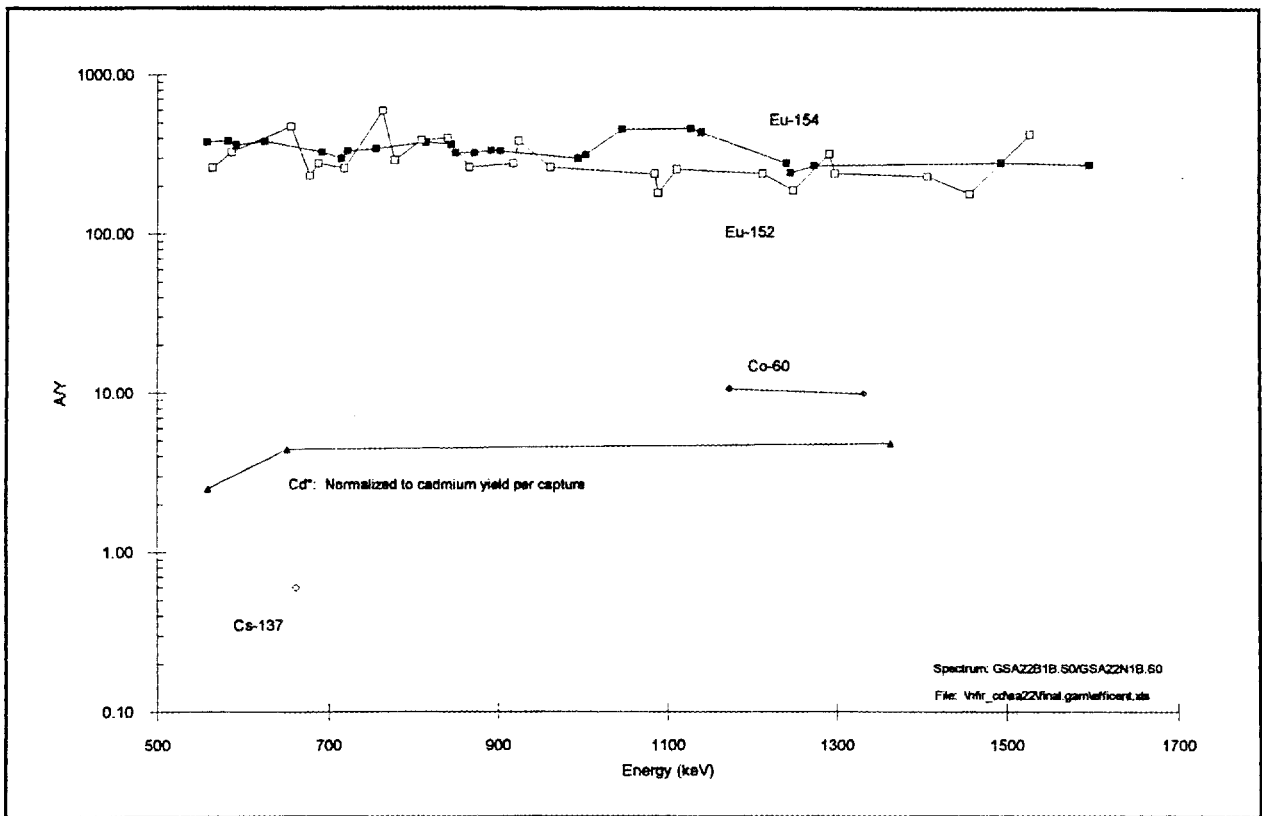


Figure 2.6. *Relative Measured Activity of Detected Isotopes*

The cadmium gamma-ray signals are also plotted on the graph, again normalized by the yield per neutron capture. The shape of the three efficiency points for Cd is consistent with the

shape of the more abundant contaminant radionuclides. Some ancillary studies with a known 1.27 mCi point source of ^{152}Eu and ^{154}Eu (exposure conversion factor of about $0.6 \text{ Rh}^{-1} \text{ Ci}^{-1}$ at 1 meter) revealed that an approximate efficiency for the detector at 558 keV is 7×10^{-4} counts per second per disintegration per second (cps/dps). Using this approximation, the measured gamma-ray count rate of 1.8 counts per second from cadmium neutron capture at 558.6 keV corresponds to about 4000 gamma-rays per second at the detector.

2.2 Neutron Transmission

2.2.1 Post

Neutron background and source measurements for the post of SA22 were acquired for a live time of 600 sec, each. This was a sufficient counting period to achieve a better than 5% counting error. The pulse height distributions for the ^3He counter are shown in Figures 2.7 and 2.8. Two regions of interest (ROI) were set in each case. ROI 1 was an integration over the entire distribution of events, except for low-energy gamma-ray interactions which were rejected via the lower level discriminator. ROI 1 was the area under the points from the $^3\text{He}(n,p)^3\text{H}$ threshold through the thermal neutron peak. ROI 2 was established to integrate only the thermal neutron peak. Two separate regions were established to monitor detector performance and stability over the measurement period. Stability was determined to be within a few percent.

The background measurement is stored in file nsa22bp.s0. For the background measurements, the number of gross events recorded in ROI 1 was 246, ROI 2 was 112.

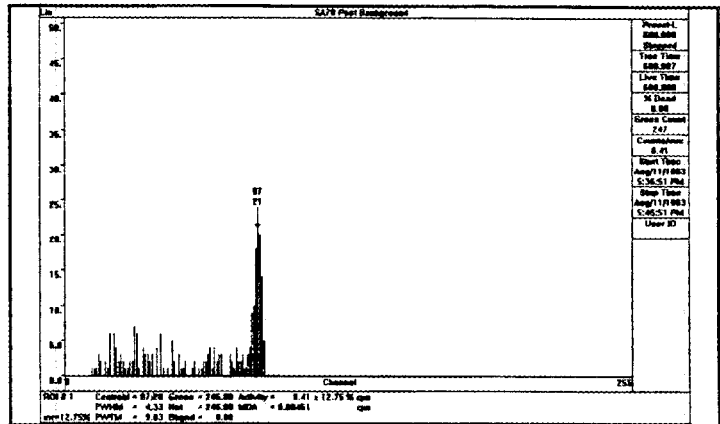


Figure 2.7. SA22 Post Neutron Background (ROI1)

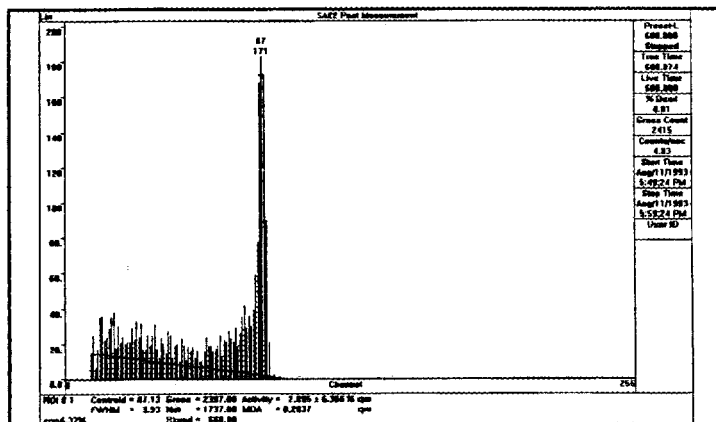


Figure 2.8. SA22 Post Neutron Measurement (ROI1)

The source measurement using a PuF_4 neutron source is stored in file nsa22cp.s0. The number of gross events recorded in ROI 1 was 2397, ROI 2 was 974.

2.2.2 Shroud

Neutron background and source measurements for the shroud of SA22 were acquired for a live time of 240 sec, each. This was a sufficient counting time to achieve better than 5% counting error. The pulse-height distributions are shown in Figures 2.9 and 2.10.

The background measurement is stored in file nsa22bs.so. The number of gross events recorded in ROI 1 was 324, ROI 2 was 131.

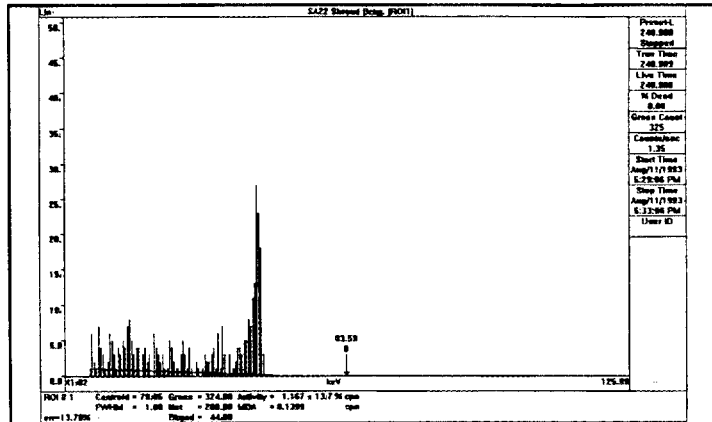


Figure 2.9. SA22 Shroud Neutron Background (ROI1)

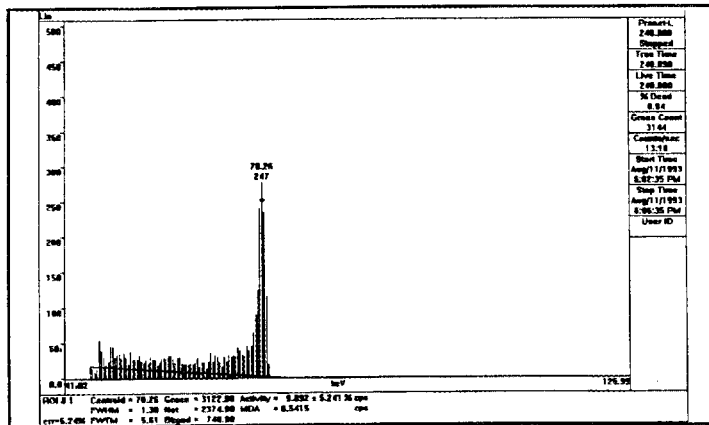


Figure 2.10. SA22 Shroud Neutron Measurement (ROI1)

The source measurement using a PuF₄ neutron source is stored in file nsa22cs.s0. The number of gross events recorded in ROI 1 was 3122, ROI 2 was 1359.

3.0 CONCLUSIONS

Measurement data support unequivocally that cadmium is present in the post and the shroud of SA22. A comparison of the shroud gamma-ray spectra for SA22, SA70, and SA00 presented in Figure 2.5 revealed that the 558.6-keV gamma-ray was observed in SA22 and SA70, but not in SA00. Accompanying cadmium-capture gamma-rays were observed in SA22 because it was measured for a longer time (2 hours). Neutron transmission was a factor of six greater in the post of SA00 than it was in either post of SA22 or SA70. Neutron transmission was a factor of ten greater in the shroud of SA00 than it was in either shroud of SA22 or SA70. The difference in the transmission factors between shrouds and posts should not be used, however, to infer cadmium thickness. Nor can the results be used for determining the uniformity of cadmium throughout a shroud assembly.

A control chart of the 558.6-keV gamma-ray production rates for test assemblies, relative to SA70, is presented in Figure 3.1. This graph will be updated as each test assembly is measured, for example, results for SA23 and SA24 will be recorded on the control chart as the measurements proceed. The 558.6-keV production rate is within 3% for SA22 and SA70; it is zero for SA00. The relative standard deviation of the ratio SA22/SA70 is less than 3%.

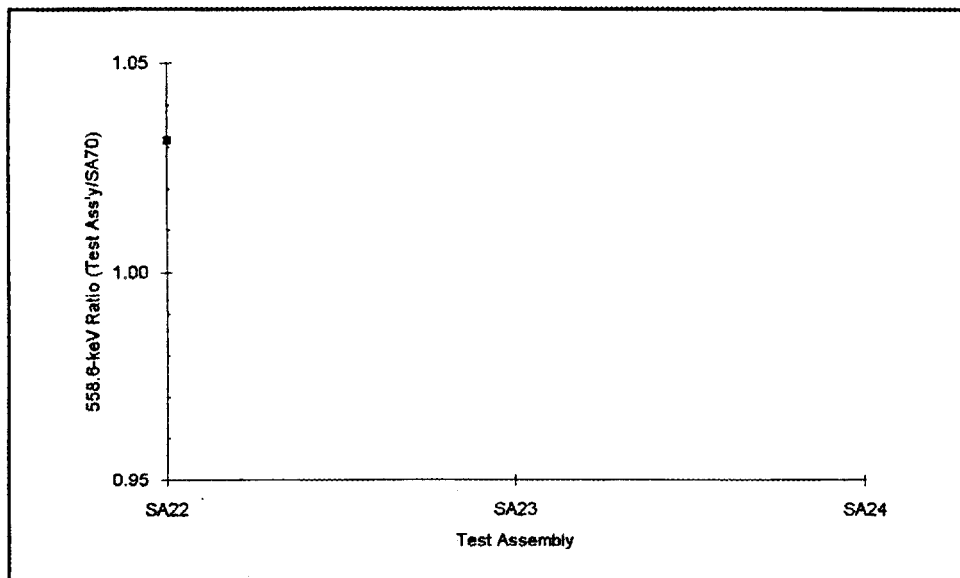


Figure 3.1 Control Chart of 558.6-keV Gamma-ray Ratios---Test Assemblies to SA70

Similarly, control charts of neutron transmission ratios for the post and shroud are presented in Figures 3.2 and 3.3, respectively. Relative transmission is indexed to both calibration assemblies---SA00 (no cadmium) and SA70 (with cadmium). Percent relative standard deviations (%RSD) are less than 3% in all cases. There is a distinguishable difference in relative flux when cadmium is present.

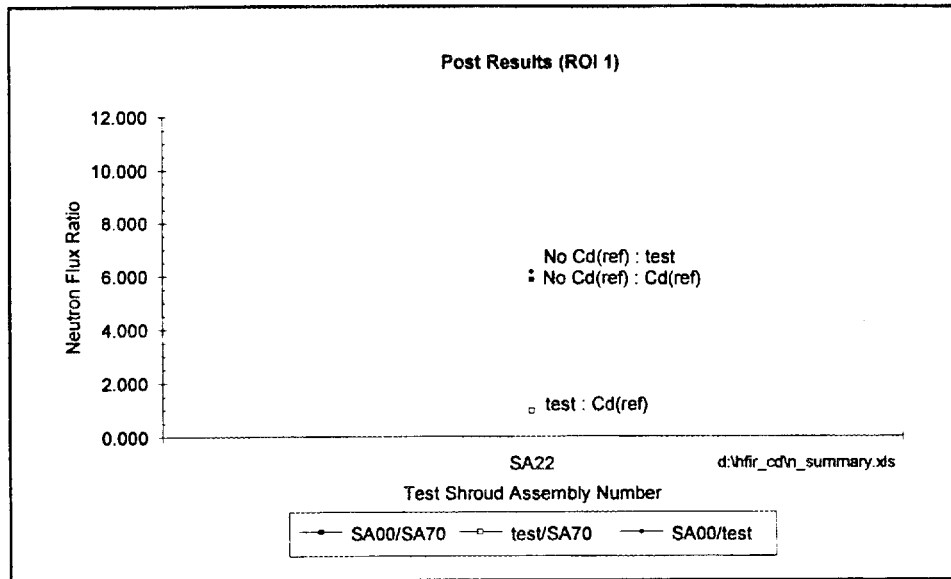


Figure 3.2. Control Chart of Neutron Flux Ratios---Test Assemblies to Calibration Assemblies (Post)

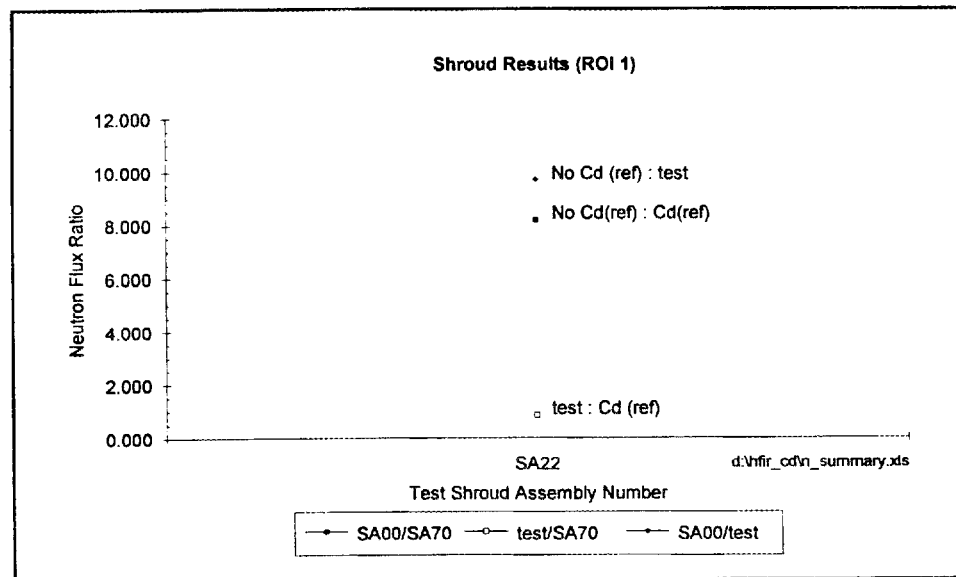


Figure 3.2. Control Chart of Neutron Flux Ratios---Test Assemblies to Calibration Assemblies (Shroud)

4.0 REFERENCES

- [1] "*Cadmium Verification of HFIR Shrouds*," Internal Correspondence/Interim Report from J.A. Chapman to D. Dabbs. Oak Ridge National Laboratory. November 11, 1992.
- [2] "*Cadmium Verification of HFIR Shroud Assemblies*," C-HFIR-92-DRAFT. High Flux Isotope Reactor Engineering Department. Oak Ridge National Laboratory. (November 15, 1992).
- [3] Chapman J.A., Schultz F.J., "*Verification of Cadmium in HFIR Spent Fuel Shroud Assemblies by Neutron-induced Gamma-ray Spectroscopy and Neutron Transmission Measurements*", ORNL/TM-12627, Waste Management Division, Oak Ridge National Laboratory, (March 31, 1994).
- [4] Etherington H., ed. "*Nuclear Engineering Handbook*", McGraw-Hill Book Company, (1958).
- [5] "*Guidebook for the ENDF/B-V Nuclear Data Files*", Brookhaven National Laboratory, EPRI NP-2510, (July 1982).
- [6] Heath R. L., "*Gamma-ray Spectrum Catalogue Ge(Li) and Si(Li) Spectrometry*," Aerojet Nuclear Company, Third Ed., TID-4500.
- [7] Jaeger R.G., Blizzard E.P., Chilton A.B., Grotenhuis M., Honig A., Haeger Th.A., Eisenholt H.H., eds. "*Engineering Compendium on Radiation Shielding*," International Atomic Energy Agency, vol. 1, Springer-Verlang, New York, (1968).
- [8] Lefort M, "*Nuclear Chemistry*", D. Van Nostrand Co. LTD, London, (1968).
- [9] Lone M.A., Leavitt R.A. and Harrison D.A., "*Prompt Gamma Rays from Thermal-Neutron Capture*," Atomic Data and Nuclear Data Tables, 26, 511-559, Academic Press, (1981).
- [10] L. Pierce to J. A. Chapman. "*AutoCad Drawings and MCS Components Used for Measuring Cadmium in HFIR Shroud*," Internal Correspondence, Oak Ridge National Laboratory. (June 1993).
- [11] "*PCMCA/WIN Manual---Basic Display and Acquisition Software*," APTEC Nuclear, Inc., ver. 4.3, (1992).
- [12] RRD Calculation C-HFIR-93-060, "*Techniques for the X-ray Analysis of HFIR Shroud Assembly*." Martin Marietta Energy Systems. HFIR Reactor Engineering Department. (October 1993).

APPENDIX A

Gamma-ray Region-of-Interest Output for SA22

This appendix is a hard-copy of the PC/MCA software output showing the region of interest statistics for identified photopeaks. It contains three parts: (1) the background photopeaks measured in the counting geometry without the ^{252}Cf source present; (2) the photopeaks resulting from a 2-hour count of the shroud with the ^{252}Cf source in place, in particular the 558.6-keV photopeak from cadmium; and (3) the output from the stripped spectrum (background + source spectrum minus the background spectrum).

The spectral data files and resulting analysis files are given below. Files with extensions of S0 are the default APTEC/MCA files saved for each measurement. Files with extension of LST are the ASCII output files for the .S0 file---these are the files presented in A.1, A.2, and A.3. Files for the gamma-ray measurements and analysis are archived in the directory D:\HFIR_CD\SA22\FINAL.GAM:

GSA22B1A	S0	33600	08-19-93	3:53p	Original Bkg. w/ CoBaCs ecal
GSA22C1A	S0	30272	08-19-93	12:55p	Original Source w/ CoBaCs ecal
GSA22B1B	S0	17504	08-20-93	2:12p	Bkg w/ intrinsic ecal
GSA22B1B	LST	15012	08-20-93	6:27p	LIST of output
GSA22B1B	LIB	10537	08-20-93	6:26p	Library analysis output
GSA22C1B	S0	30288	08-20-93	2:11p	Source w/ intrinsic ecal
GSA22C1B	LST	15604	08-20-93	6:30p	LIST of output
GSA22C1B	LIB	10850	08-20-93	6:30p	Library analysis output
GSA22N1B	S0	19024	08-20-93	3:54p	NET Spectrum (S-B)
GSA22N1B	LST	2963	08-20-93	6:33p	LIST of output
GSA22N1B	LIB	6270	08-20-93	6:32p	Library analysis output
GSA22RLT	WRI	72192	08-21-93	9:14a	.WRI file of ResuLTs
README	JAC	1811	08-21-93	10:05a	This readme file

A.1 Shroud Gamma-ray Background Spectrum

File: GSA22B1B.LST

Aptec PC/MCA Spectrum Printout Aug/20/1993 6:26:33 pm

HFIR SHROUD PROJECT

SA22 2-hr BKG. 8/19 self-ecal

Identification	Acquisition
File : MCARD#1.S00	Started : Aug/19/1993 1:24:57 pm
User :	Stopped : Aug/19/1993 3:41:45 pm
MCard : 1	True : 8207.89 sec
Detector :	Live : 7200.00 sec
Geometry :	Dead : 12.28 %
Sample :	Gross Count : 20904700 counts
Channels : 4096	Gross Rate : 2903 cps

Sample

A.1 Shroud Gamma-ray Background Spectrum (continued)

Energy Calibration Time : Aug/20/1993 10:36:36 am
 E = 5.551 + 0.3930C

Errors Quoted at 2 Sigma
 MDA's Quoted at 1.645 Sigma

ACTIVITY INFORMATION

Name	- Library	Energy keV Measured	L - M	FWHM	- Activity cps	Error
Annih	511.00	511.00	-0.00	2.90	2.170	±0.216
Co-60	1173.23	1173.21	0.02	1.87	10.67	±0.132
Co-60	1332.51	1332.49	0.02	1.94	9.985	±0.103
Cs-137	661.62	661.35	0.27	1.97	0.5078	±0.147
Eu-152	564.00	563.78	0.22	1.44	1.258	±0.148
Eu-152	586.30	586.20	0.10	1.64	1.475	±0.15
Eu-152	656.40	656.44	-0.04	1.83	0.6656	±0.169
Eu-152	678.60	678.32	0.28	1.34	1.096	±0.165
Eu-152	688.60	688.47	0.13	1.62	2.341	±0.164
Eu-152	719.30	719.27	0.03	1.48	0.7008	±0.125
Eu-152	764.80	764.79	0.01	2.01	1.009	±0.166
Eu-152	778.89	778.96	-0.07	1.61	37.01	±0.259
Eu-152	810.40	810.35	0.05	1.65	1.207	±0.154
Eu-152	841.50	840.90	0.60	2.12	0.6402	±0.136
Eu-152	867.32	867.48	-0.16	1.70	10.97	±0.162
Eu-152	919.30	919.55	-0.25	1.83	1.111	±0.127
Eu-152	926.30	926.03	0.27	2.22	1.001	±0.13
Eu-152	964.01	964.17	-0.16	1.71	37.97	±0.217
Eu-152	1085.80	1085.82	-0.02	1.78	23.91	±0.165
Eu-152	1089.70	1089.79	-0.09	1.68	3.060	±0.116
Eu-152	1112.00	1112.01	-0.01	1.82	34.13	±0.204
Eu-152	1212.80	1212.96	-0.16	1.90	3.336	±0.0911
Eu-152	1249.80	1250.00	-0.20	1.93	0.3416	±0.0595
Eu-152	1292.70	1292.93	-0.23	2.29	0.3201	±0.0681
Eu-152	1299.00	1299.16	-0.16	1.98	3.887	±0.0871
Eu-152	1408.00	1408.02	-0.02	2.00	48.06	±0.179
Eu-152	1457.50	1457.57	-0.07	1.89	0.8844	±0.0467
Eu-152	1528.10	1528.89	-0.79	3.27	1.107	±0.0467
Eu-154	557.60	557.50	0.10	1.59	0.9872	±0.146
Eu-154	582.00	581.92	0.08	1.56	3.234	±0.173
Eu-154	591.80	591.59	0.21	1.45	17.55	±0.24
Eu-154	625.20	624.79	0.41	1.47	1.188	±0.172
Eu-154	692.40	692.41	-0.01	1.54	5.533	±0.164
Eu-154	715.80	715.58	0.22	1.93	0.5090	±0.124
Eu-154	723.30	723.23	0.07	1.56	65.48	±0.275
Eu-154	756.90	756.82	0.08	1.59	14.86	±0.228
Eu-154	815.60	815.62	-0.02	1.60	1.776	±0.141
Eu-154	845.40	845.65	-0.25	1.86	2.011	±0.138
Eu-154	850.60	850.83	-0.23	1.48	0.7448	±0.125
Eu-154	873.20	873.31	-0.11	1.65	36.69	±0.214
Eu-154	892.70	892.86	-0.16	1.67	1.546	±0.122
Eu-154	904.10	904.47	-0.37	1.57	2.724	±0.161
Eu-154	996.30	996.34	-0.04	1.73	30.81	±0.199
Eu-154	1004.80	1004.85	-0.05	1.76	56.51	±0.258
Eu-154	1047.40	1047.55	-0.15	2.16	0.6376	±0.137
Eu-154	1128.40	1128.07	0.33	1.87	1.246	±0.126
Eu-154	1140.90	1140.94	-0.04	2.24	0.9629	±0.107
Eu-154	1241.60	1241.46	0.14	1.54	0.3656	±0.0643
Eu-154	1246.20	1246.16	0.04	1.79	2.200	±0.0768
Eu-154	1274.80	1274.48	0.32	1.92	95.89	±0.258
Eu-154	1494.60	1494.04	0.56	2.11	1.889	±0.0521
Eu-154	1597.30	1596.53	0.77	2.13	4.672	±0.0634

A.1 Shroud Gamma-ray Background Spectrum (continued)

PEAKS NOT IDENTIFIED

ROI (#)	Centroid keV	FHWM keV	Net Count Rate cps	Error
1	502.44	3.17	8.564	±0.163
9	649.11	1.50	0.6446	±0.158
28	880.58	2.11	0.3919	±0.107
42	1151.97	2.42	0.7053	±0.102
44	1188.30	2.43	0.3454	±0.0933
46	1233.96	2.28	0.3435	±0.0721
53	1317.09	2.33	0.4015	±0.0646
55	1349.03	2.47	0.2093	±0.0588
56	1397.55	1.97	0.8948	±0.0564
58	1447.57	2.42	0.7367	±0.0573
62	1537.86	2.07	0.1822	±0.037

A.2 Shroud Gamma-ray Spectrum with ²⁵²Cf Source

File: GSA22C1B.LST

Aptec PC/MCA Spectrum Printout Aug/20/1993 6:30:07 pm

HFIR SHROUD PROJECT

SA22 2-hr SOURCE 8/19 self-ecal

Identification		Acquisition	
File	: MCARD#1.S00	Started	: Aug/19/1993 10:16:50 am
User	:	Stopped	: Aug/19/1993 12:35:50 pm
MCard	: 1	True	: 8339.57 sec
Detector	:	Live	: 7200.00 sec
Geometry	:	Dead	: 13.66 %
Sample	:	Gross Count	: 23099640 counts
Channels	: 4096	Gross Rate	: 3208 cps

Analysis Flags	Aquisition Flags
Divided By Efficiency	

Energy Calibration Time : Aug/20/1993 10:30:54 am
E = 6.409 + 0.3923C

Errors Quoted at 2 Sigma
MDA's Quoted at 1.645 Sigma

ACTIVITY INFORMATION

Name	- Library	Energy keV Measured	L - M	FHWM	- Activity cps	Error
Annih	511.00	511.11	-0.11	2.95	4.680	±0.253
Co-60	1173.23	1173.12	0.11	1.87	10.55	±0.155
Co-60	1332.51	1332.53	-0.02	1.99	10.12	±0.115
Cs-137	661.62	661.52	0.10	1.47	1.572	±0.163
Eu-152	564.00	564.52	-0.52	1.57	1.800	±0.219
Eu-152	586.30	586.15	0.15	1.27	1.076	±0.16
Eu-152	656.40	656.59	-0.19	2.01	0.6519	±0.173
Eu-152	678.60	678.28	0.32	1.59	1.352	±0.183
Eu-152	688.60	688.59	0.01	1.55	2.271	±0.148
Eu-152	719.30	719.25	0.05	1.36	0.7459	±0.123
Eu-152	764.80	764.52	0.28	1.58	0.8565	±0.17
Eu-152	778.89	778.91	-0.02	1.58	36.35	±0.264
Eu-152	810.40	810.32	0.08	1.71	1.108	±0.142
Eu-152	841.50	841.13	0.37	0.90	0.5395	±0.133
Eu-152	867.32	867.41	-0.09	1.71	10.69	±0.176
Eu-152	919.30	919.56	-0.26	1.58	1.097	±0.139

A.2 Shroud Gamma-ray Spectrum with ²⁵²Cf Source (continued)

Name	Energy keV			FWHM	Activity cps	Error
	Library	Measured	L - M			
Eu-152	926.30	925.85	0.45	2.90	1.032	±0.137
Eu-152	964.01	964.06	-0.05	1.77	37.67	±0.232
Eu-152	1085.80	1085.75	0.05	1.77	23.74	±0.169
Eu-152	1089.70	1089.69	0.01	1.63	2.913	±0.124
Eu-152	1112.00	1112.01	-0.01	1.83	33.35	±0.196
Eu-152	1212.80	1212.92	-0.12	1.93	3.360	±0.112
Eu-152	1249.80	1250.44	-0.64	1.72	0.4060	±0.0819
Eu-152	1292.70	1292.55	0.15	2.02	0.3424	±0.0835
Eu-152	1299.00	1299.11	-0.11	1.95	3.766	±0.0952
Eu-152	1408.00	1408.10	-0.10	2.04	47.00	±0.183
Eu-152	1457.50	1457.70	-0.20	1.92	0.8260	±0.053
Eu-152	1528.10	1528.95	-0.85	3.68	1.253	±0.0616
Eu-154	557.60	558.19	-0.59	1.78	3.030	±0.209
Eu-154	582.00	581.97	0.03	1.62	3.284	±0.176
Eu-154	591.80	591.71	0.09	1.51	16.44	±0.211
Eu-154	625.20	625.33	-0.13	1.65	1.170	±0.158
Eu-154	692.40	692.42	-0.02	1.51	5.614	±0.178
Eu-154	715.80	714.92	0.88	1.89	1.022	±0.173
Eu-154	723.30	723.28	0.02	1.57	64.87	±0.291
Eu-154	756.90	756.78	0.12	1.65	14.05	±0.213
Eu-154	815.60	815.49	0.11	1.64	1.982	±0.166
Eu-154	845.40	845.92	-0.52	2.60	2.814	±0.157
Eu-154	850.60	850.95	-0.35	1.70	0.7136	±0.147
Eu-154	873.20	873.27	-0.07	1.71	36.00	±0.225
Eu-154	892.70	892.78	-0.08	1.75	1.615	±0.159
Eu-154	904.10	904.29	-0.19	1.61	2.340	±0.154
Eu-154	996.30	996.33	-0.03	1.76	30.30	±0.212
Eu-154	1004.80	1004.73	0.07	1.77	54.90	±0.259
Eu-154	1047.40	1047.71	-0.31	2.01	0.5368	±0.129
Eu-154	1128.40	1127.87	0.53	1.87	1.087	±0.126
Eu-154	1140.90	1140.68	0.22	2.01	0.8114	±0.0992
Eu-154	1241.60	1241.20	0.40	1.74	0.3090	±0.0653
Eu-154	1246.20	1246.12	0.08	1.83	2.033	±0.086
Eu-154	1274.80	1274.40	0.40	1.95	94.26	±0.266
Eu-154	1494.60	1494.22	0.38	2.14	1.832	±0.0654
Eu-154	1597.30	1596.84	0.46	2.17	4.835	±0.0731

PEAKS NOT IDENTIFIED

ROI (#)	Centroid keV	FWHM keV	Net Count Rate cps	Error	
1	502.83	3.65	12.77	±0.181	
3	535.88	1.61	0.7304	±0.217	
10	650.13	0.74	0.6135	±0.18	Cd*
24	835.78	2.35	0.5056	±0.147	
34	931.04	1.36	0.4327	±0.127	
44	1151.70	1.99	0.6747	±0.113	
46	1188.83	1.58	0.6212	±0.1	
48	1233.53	1.33	0.2903	±0.0803	
55	1317.03	1.72	0.2657	±0.0647	
57	1364.39	2.11	0.2403	±0.0646	Cd*
58	1397.84	2.19	0.9707	±0.0684	
60	1435.61	2.55	0.3728	±0.0606	
61	1448.02	2.26	0.6610	±0.062	
65	1538.28	2.94	0.2323	±0.0445	

A.3 Stripped Gamma-ray Spectrum

File: GSA22N1B.LST

Aptec PC/MCA Spectrum Printout Aug/20/1993 6:33:05 pm

HFIR SHROUD PROJECT

SA22 2-hr 8/19 ***Stripped***

Identification	Acquisition
File : MCARD#1.S00	Started : Aug/19/1993 10:16:50 am
User :	Stopped : Aug/19/1993 12:35:50 pm
MCArd : 1	True : 131.67 sec
Detector :	Live : 0.00 sec
Geometry :	Dead : 100.00 %
Sample :	Gross Count : 2195624 counts
Channels : 4096	Gross Rate : 0 cps

Analysis Flags	Aquisition Flags
Spectrum was Stripped	
Spectrum was Smoothed (3 point)	

Energy Calibration Time : Aug/20/1993 10:30:54 am

Errors Quoted at 2 Sigma
MDA's Quoted at 1.645 Sigma

ROI COUNT INFORMATION

ROI (#)	Channels Start - Stop	Energy keV Start - Stop	Net Counts	Background Counts	Gross Counts
1	1257 - 1275	499.38 - 506.44	19518	6978	26496
2	1275 - 1302	506.44 - 517.03	36023	33863	69886
3	1400 - 1420	555.45 - 563.29	13223	34386	47609
4	1912 - 1925	756.18 - 761.28	8229	5850	14079
5	2973 - 2988	1172.04 - 1177.92	5921	2988	8909
6	4054 - 4078	1595.59 - 1604.99	6115	3406	9521

ROI STATISTICS INFORMATION

ROI (#)	Error	Centroid keV	FWHM keV	FWTM keV	FWTM/FWHM ratio	H/L ratio
1	1.87 %	503.83				
2	1.79 %	510.69	5.29			
3	4.33 %	558.47	2.23	4.05	1.82	5.234/5.104
4	3.43 %	758.52	2.43	4.61	1.90	6.918/4.842
5	3.68 %	1174.77	2.26			
6	3.72 %	1598.04	2.56	7.93	3.09	15.25/4.996

ACTIVITY INFORMATION

Name	Library	Energy keV Measured	L - M	FWHM	Activity cps	Error
Annih	511.00	510.69	0.31	5.29	0.0000	
Cd	558.60	558.47	0.13	2.23	0.0000	

APPENDIX B

Neutron Region-of-Interest Output for SA22

This appendix is a hard-copy of the PC/MCA software output showing the two regions of interest statistics for pulse height distributions recorded from the ^3He neutron detector. A background measurement was made for the shroud and then the post; the source-count measurements were performed thereafter.

The spectral data files and resulting analysis files are given below. Files with extensions of S0 are the default APTEC/MCA files saved for each measurement. Files with extension of LST are the ASCII output files for the .S0 file. Files for the neutron measurements and analysis are archived in the directory D:\HFIR_CD\SA22\FINAL.NUT:

```
D:\hfir_cd\sa22\final.nut\readme.jac
NSA22BS S0      2584 08-11-93  5:33p Background of the shroud
NSA22BS WRI    36096 08-11-93  5:33p
NSA22BS LST    1463 08-11-93  5:34p

NSA22BP S0      2584 08-11-93  5:46p Background of the post
NSA22BP WRI    36096 08-11-93  5:47p
NSA22BP LST    1495 08-11-93  5:47p

NSA22CP S0      2584 08-11-93  5:59p Count of the post
NSA22CP WRI    36096 08-11-93  6:00p
NSA22CP LST    1495 08-11-93  6:00p

NSA22CS S0      2584 08-11-93  6:07p Count of the shroud
NSA22CS WRI    36096 08-11-93  6:08p
NSA22CS LST    1525 08-11-93  6:09p
```

File-NSA22BS.LST

Aptec PC/MCA Spectrum Printout Aug/11/1993 5:34:05 pm

Identification	Acquisition
File : MCARD#1.S00	Started : Aug/11/1993 5:29:06 pm
User :	Stopped : Aug/11/1993 5:33:06 pm
MCard : 1	True : 240.01 sec
Detector :	Live : 240.00 sec
Geometry :	Dead : 0.00 %
Sample :	Gross Count : 325 counts
Channels : 256	Gross Rate : 1.354 cps

Sample

Energy Calibration Time : Aug/5/1993 11:10:33 am

Errors Quoted at 2 Sigma
MDA's Quoted at 1.645 Sigma

ROI COUNT INFORMATION

ROI (#)	Channels Start - Stop	Energy keV Start - Stop	Net Counts	Background Counts	Gross Counts
1	11 - 97	44.67 - 73.26	280	44	324
2	78 - 97	66.94 - 73.26	89	42	131

File-NSA22CS.LST

Aptec PC/MCA Spectrum Printout Aug/11/1993 6:09:04 pm

Identification	Acquisition
File : MCARD#1.S00	Started : Aug/11/1993 6:02:35 pm
User :	Stopped : Aug/11/1993 6:06:35 pm
MCArd : 1	True : 240.10 sec
Detector :	Live : 240.00 sec
Geometry :	Dead : 0.04 %
Sample :	Gross Count : 3144 counts
Channels : 256	Gross Rate : 13.1 cps

Sample

Energy Calibration Time : Aug/5/1993 11:10:33 am

Errors Quoted at 2 Sigma
MDA's Quoted at 1.645 Sigma

ROI COUNT INFORMATION

ROI (#)	Channels Start - Stop	Energy keV Start - Stop	Net Counts	Background Counts	Gross Counts
1	11 - 97	44.67 - 73.26	2374	748	3122
2	78 - 97	66.94 - 73.26	960	399	1359

File-NSA22BP.LST

Aptec PC/MCA Spectrum Printout Aug/11/1993 5:47:39 pm

Identification	Acquisition
File : MCARD#1.S00	Started : Aug/11/1993 5:35:51 pm
User :	Stopped : Aug/11/1993 5:45:51 pm
MCArd : 1	True : 600.01 sec
Detector :	Live : 600.00 sec
Geometry :	Dead : 0.00 %
Sample :	Gross Count : 247 counts
Channels : 256	Gross Rate : 0.4117 cps

Sample

Energy Calibration Time : Aug/5/1993 11:10:33 am

Errors Quoted at 2 Sigma
MDA's Quoted at 1.645 Sigma

ROI COUNT INFORMATION

ROI (#)	Channels Start - Stop	Energy keV Start - Stop	Net Counts	Background Counts	Gross Counts
1	11 - 97	44.67 - 73.26	246	0	246
2	78 - 97	66.94 - 73.26	91	21	112

File-NSA22CP.LST

Aptec PC/MCA Spectrum Printout Aug/11/1993 6:00:32 pm

Identification		Acquisition	
File	: MCARD#1.S00	Started	: Aug/11/1993 5:49:24 pm
User	:	Stopped	: Aug/11/1993 5:59:24 pm
MCard	: 1	True	: 600.07 sec
Detector	:	Live	: 600.00 sec
Geometry	:	Dead	: 0.01 %
Sample	:	Gross Count	: 2415 counts
Channels	: 256	Gross Rate	: 4.025 cps

Sample

Energy Calibration Time : Aug/5/1993 11:10:33 am

Errors Quoted at 2 Sigma
MDA's Quoted at 1.645 Sigma

ROI COUNT INFORMATION

ROI (#)	Channels Start - Stop	Energy keV Start - Stop	Net Counts	Background Counts	Gross Counts
1	11 - 97	44.67 - 73.26	1737	660	2397
2	78 - 97	66.94 - 73.26	607	368	974

APPENDIX C

Analysis Worksheet

The two attached sheets are from the Microsoft EXCEL™ spreadsheet that was designed for entering the raw data, computing and propagating the error (see ref. 3 for methods), tallying the results, and plotting the cumulative gamma-ray and neutron transmission data as observed in Figures 3.1 through 3.3. The first page provides cells for entering the raw data. Gray-shaded cells have been programmed to compute the error terms. The second page reads the raw data from page one and prints the results. The results are then read by a routine that plots ratios of the 558.6-keV gamma-ray yields (test assembly to SA70), and neutron transmission ratios in the post and shroud.

HFIR SHROUD CADMIUM VERIFICATION MEASUREMENTS

SA22

Waste Examination and Assay Facility

Oak Ridge National Laboratory

Basic Data

Shroud Assembly No: SA22	Date of Assay: 8/11/93(ref) 8/19/93(SA22)
Date of Receipt: Jul-93	Dose rate @ contact (mR/h): 2

Quality Control

check

Perform neutron source check of 3He detector (before/after)	x
Perform energy calibration of HPGe detector (before/after)	x

Measurement Data

<i>n</i> -transmission		Measured Neutron Flux (counts)					
		SA00 std (no Cd)		SA70 std (Cd)		SA22	
		mean	stdev.	mean	stdev.	mean	stdev.
SHROUD (4-min)							
Bckg. (B)	ROI1	442	21.02	151	12.29	324	18.00
	ROI2	188	13.71	54	7.35	131	11.45
Source (S)	ROI1	27607	166.15	3470	58.91	3122	55.87
	ROI2	11727	108.29	1528	39.09	1359	36.86
S-B	ROI1	27165.00	167.48	3319.00	60.17	2755.00	58.70
	ROI2	11539.00	109.16	1474.00	39.77	1228.00	38.60
QC: ROI1/ROI2		2.35		2.25		2.28	
POST (10-min)							
Bckg. (B)	ROI1	839	28.97	237	15.39	246	15.68
	ROI2	338	18.38	79	8.89	112	10.58
Source (S)	ROI1	14090	118.70	2499	49.99	2397	48.96
	ROI2	5837	76.40	1014	31.84	974	31.21
S-B	ROI1	13251.00	122.18	2262.00	52.31	2151.00	61.41
	ROI2	5499.00	78.58	935.00	33.06	862.00	32.95
QC: ROI1/ROI2		2.41		2.42		2.50	
<i>Prompt gamma-ray spectroscopy</i>		Measured Gamma-ray Activity (counts per sec)					
		SA00 std (no Cd)		SA70 std (Cd)		SA22	
		mean	error (2s)	mean	error (2s)	mean	error (2s)
SHROUD (20-min)							
Bckg. (B)	keV						
Eu154	ROI2-557.6					0.99	0.15
Eu154	ROI3-592					17.55	0.24
Cd*	ROI3-651.3						
Eu152	ROI4-779	0.16	0.04	0.21	0.04	37.01	0.26
Eu154	ROI5-873	0.13	0.03	0.15	0.04	36.69	0.21
Eu154	ROI6-996	0.14	0.03	0.13	0.03	30.81	0.20
Eu152	ROI7-1112	0.35	0.04	0.35	0.04	34.13	0.20
Co60	ROI8-1333	0.15	0.03	0.17	0.03	9.98	0.10
Eu152	ROI9-1408	0.81	0.05	0.80	0.05	48.06	0.18
Source (S)							
Cd*	ROI1-658.6	0	0	1.78	0.14	1.84	0.03
Eu154	ROI2-592					16.44	0.21
Cd*	ROI3-651.3					0.61	0.18
Eu152	ROI4-779					36.35	0.26
Eu154	ROI5-873					36.00	0.22
Eu154	ROI6-996					30.30	0.21
Eu152	ROI7-1112	0.48	0.08	0.44	0.07	33.35	0.20
Co60	ROI8-1333	0.23	0.06	0.20	0.05	10.12	0.12
Cd*	ROI9-1364.3					0.24	0.06
Eu152	ROI10-1408	0.96	0.08	0.82	0.07	47.00	0.18

Measurement Results

<i>n</i> -transmission	Neutron Transmission Ratios					
	SA00/SA70		SA00/SA22		SA22/SA70	
	mean	stdev.	mean	stdev.	mean	stdev.
SHROUD (4-min)						
Bckg. (B) ROI1	2.93	0.28	1.36	0.10	2.15	0.21
Source (S) ROI1	7.96	0.14	8.84	0.17	0.90	0.02
S-B ROI1	8.18	0.16	9.71	0.21	0.84	0.02
Relative % Std. Dev.		1.91%		2.19%		2.77%
POST (10-min)						
Bckg. (B) ROI1	3.54	0.26	3.41	0.25	1.04	0.09
Source (S) ROI1	5.64	0.12	5.88	0.13	0.96	0.03
S-B ROI1	5.86	0.15	6.16	0.16	0.95	0.03
Relative % Std. Dev.		2.49%		2.56%		3.33%

Comment: SA22 is more absorbing than SA70

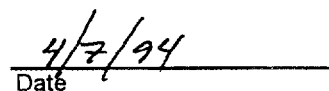
<i>n</i> -transmission	Shroud to Post Comparison					
	Post			Shroud		
	SA22	SA70	SA00	SA22	SA70	SA00
Neutron count rate (1/sec)	3.59	3.77	22.09	11.66	13.83	113.19
+/- 1s	0.08	0.08	0.19	0.22	0.24	0.69
Nominal thickness Cd (in.)	0.058	0.036	0.000	0.036	0.036	0.000
During meas. Cd, t (in.)*	0.116	0.072	0.000	0.036	0.036	0.000
Density-thickness (g/cm ²)	1.36E+22	8.43E+21	0.00E+00	4.21E+21	4.21E+21	0.00E+00
exp(-capsig*t)	3.57E-15	1.08E-09	1.00E+00	3.28E-05	3.28E-05	1.00E+00
Src-det. distance, r (in)	10	10	10	6	6	6
Neutron count rate (1/r ²)	9.96	10.47	61.35	4.20	4.98	40.75

* Nominal Cd thickness in post counting geometry is "double layer"

<i>n</i> -transmission	Shroud to Post Ratios			
	SA22	SA70	SA00	Comments
Neutron count rates	3.25	3.67	5.13	SA70>SA22, SA00>>SA70 and 22
std. dev. (s)	0.09	0.10	0.05	
Account for r ⁻²	1.17	1.32	1.85	

Prompt gamma-ray spectroscopy	Ratios of Cadmium Photopeaks		
	SA00/SA70	SA00/SA22	SA22/SA70
Cd* ROI2-558	0.00	0.00	1.03


Signature


Date

INTERNAL DISTRIBUTION

1. T. J. Abraham
2. P. E. Arakawa
3. R. D. Bailey
4. J. S. Baldwin
5. P. T. Barton
6. M. L. Bauer
7. J. S. Bogard
8. R. Brandenburg
9. T. W. Burwinkle
10. V. R. Cain
11. D. E. Coffey
12. G. R. Cunningham
13. N. Cutshall
14. R. D. Dabbs
15. D. D. Drake
16. K. G. Edgemon
17. K.R. Elam
18. D. M Ferren
19. M. K. Ford
20. J. R. Forgy
21. C. E. Frye
22. H. R. Gaddis
23. R. B. Gammage
24. G. D. Hackett
25. R. Hagenauer
26. D. F. Hall
27. H. J. Hall
28. R. E. Halliburton
29. D. C. Hensley
30. L. Holder
31. R. J. Hydzik
32. J. K. Keith
33. G. R. Larson
34. T. Madden
35. J. E. Madison
36. A. P. Malinauskas
37. C. A. Manrod
38. R. C. Mason
39. R. Mayer
40. B. C. McClelland
41. L. E. McNeese
42. S.G. Melton
43. J. C. Nix
44. J. C. Patterson
45. Paul S. Rohwer
46. T. H. Row
47. T. F. Scanlan
48. C. B. Scott
49. J. A. Setaro
50. R. C. Stewart
51. L. E. Stratton
52. J.H. Swanks
53. J. Trabalka
54. M. W. Tull
55. D. W. Turner
56. J.E. Turner
57. J. Westbrook
58. R. L. White
59. S. E. Williams
60. P. C. Womble
61. K. G. Young
62. ORNL Patent Section
63. Central Research Library
64. Document Reference Section
- 65-66. Laboratory Records
67. Laboratory Records, ORNL-RC

EXTERNAL DISTRIBUTION

68. Andor Andrasi
KFKI Health Physics Dept.
P.O. Box 49
H-1525 Budapest Hungary
69. Fred Alberg
Martin Marietta Specialty Components
Largo, FL 34649-2908
70. Roger Allman
Nuclear Fuel Services
205 Banner Hill Road
Erwin, TN 37650
71. Greg K. Becke
EG&G Idaho, Inc.
P. O. Box 1625
Idaho Falls, Idaho 83415-2114
72. J. Mike Bieri
Pajarito Scientific Corp.
278 DP Road
Los Alamos, New Mexico 87544
73. John T. Caldwell
Pajarito Scientific Corporation
278 DP Road
Los Alamos, New Mexico 87544
74. David Camp
Lawrence Livermore National Laboratory
P.O. Box 808
Livermore, California 94550
75. Tom Clements
EG&G Idaho, Inc.
P. O. Box 1625
Idaho Falls, ID 83415
76. Don Close
Los Alamos National Laboratory
P.O. Box 1663
Los Alamos, New Mexico 87545
77. Jeff Cook
EG&G Idaho, Inc.
P. O. Box 1625
Idaho Falls, Idaho 83415-2209
78. Ken Coop
Los Alamos National Laboratory
P. O. Box 1663 N-2, MS J562
Los Alamos, New Mexico 87545
79. Larry East
EG&G Idaho, Inc.
P. O. Box 1625
Idaho Falls, Idaho 83415
80. Martin Edelson
Ames Laboratory
Iowa State University
Ames, IA 50011
81. Robert Estep
Los Alamos National Laboratory
P. O. Box 1663
Los Alamos, New Mexico 87545-J562
82. Paul Fehlau
Los Alamos National Laboratory
P. O. Box 1663
Los Alamos, New Mexico 87545-J562
83. Paul Frame
ORISE
Post Office Box 117
Oak Ridge, TN 37831-0117
84. Ann Gibbs
Westinghouse Savannah River Co.
P. O. Box 616, Building 707-C
Aiken, South Carolina 29802
85. Bill Gilles
Westinghouse Hanford Corporation
P.O. Box 1970, A1-10
Richland, Washington 99352

86. Richard A. Hamilton
Westinghouse Hanford Company
P.O. Box 1970 / MSIN T5-06
Richland, Washington 99352
87. Richard A. Hane
Westinghouse Savannah River Co.
P. O. Box 616 724-9E
Aiken, South Carolina 29802
88. Yale Harker
EG&G Idaho, Inc.
P. O. Box 1625
Idaho Falls, Idaho 83415-7113
89. Ron A. Harlan
EG&G, Rocky Flats, Inc.
P. O. Box 464 MS-881
Golden, Colorado 80402-0464
90. Ralph Hemmer
EG&G Rocky Flats, Inc.
P. O. Box 464 MS-T371D
Golden, Colorado 80402-0464
91. Paul J. Hurley
Special Technologies Laboratory
5520 Ekwill Street, Suite B
Santa Barbara, CA 93111
92. T. Kerlin
University of Tennessee
Pasqua Engineering Bldg.
Knoxville, TN 37996-2300
93. Joseph J. Kehayias
United States Depart. of Agriculture
711 Washington St.
Boston, MA 02111
94. Fred Kline
Martin Marietta Specialty Components
Largo, FL 34649-2908
95. Cecilia Lemons
Batelle, Pacific Northwest Laboratory
P.O. Box 999 M/S K3-70
Richland, WA 99352
96. Richard Lipinski
Westinghouse Hanford
P.O. Box 1970 T3-04
Richland, Washington 99352
97. Steve Lusnia
Martin Marietta Specialty Components
Largo, FL 34649-2908
98. Charlie Marcinkiewicz
Contech, Inc.
11278 Panorama Dr.
New Market, MD 21774
99. Harry E. Martz, Jr.
Lawrence Livermore National Laboratory
P.O. Box 808, L-333
Livermore, California 94551
100. Charles D. Massey
Sandia National Laboratories
P.O. Box 5800, Division 3222
Albuquerque, New Mexico 87185
101. Chuck Mikesell
EG&G Idaho, Inc.
P. O. Box 1625
Idaho Falls, Idaho 83415
102. L. Miller
University of Tennessee
Pasqua Engineering Bldg..
Knoxville, TN 37996-2300
103. C. Dennis Morissette
Westinghouse Electric Corporation
P.O. Box 2078
Carlsbad, New Mexico 88221-2078
104. John Moore
1500 Gallatin Place
Oxnard, CA 93030
105. Dan Osetek
Los Alamos Technical Associates, Inc.
2400 Louisiana N.E.
Albuquerque, NM 87110
106. Mark Pikrell
Los Alamos National Laboratory
P.O. Box 1663
Los Alamos, New Mexico 87545

107. Kim Piper
Battelle, Pacific National Lab.
P.O. Box 999
Richland, WA 99352
108. Don Pound
EG&G Idaho, Inc.
P. O. Box 1625
Idaho Falls, Idaho 83415-4203
109. Mike Purcell
Westinghouse Hanford Corporation
P. O. Box 1970, T6-16
Richland, Washington 99352
110. Bruce Reich
Los Alamos National Laboratory
P.O. Box 1663
Los Alamos, New Mexico 87545
111. L. C. M. Roddye
DOE-OR
FOB RM 2116
Oak Ridge, TN 37830
112. Jim Rowles
EG&G Las Vegas
P.O. Box 912, C1-102
Las Vegas, NV 89125
113. Joe Shappell
Savannah River Plant
Building 703-H
Aiken, South Carolina 29808
114. David Simpson
ORISE
Post Office Box 117
Oak Ridge, TN 37831-0117
115. Mark A. Smith
SAIC
301 Laboratory Rd.
Oak Ridge, TN 37830
116. Tom Snowden
Martin Marietta Specialty Components
Largo, FL 34649-2908
117. Jim Sprinkle
N-1, MS-E540
Los Alamos National Laboratory
Los Alamos, New Mexico 87545
118. Robert J. Tuttle
Rockwell International
6633 Canoga Ave.
Canoga Park, CA 91303
119. George Vourvopoulos
Department of Physics and Astronomy
Western Kentucky University
Bowling Green, Kentucky 42101
120. Joe Wachter
Los Alamos National Laboratory
P.O. Box 1663
Los Alamos, New Mexico 87545
121. J. H. Weinlein
Sandia National Laboratories
P.O. Box 5800, Division 2364
Albuquerque, New Mexico 87185
122. Bill Weston
Westinghouse Electric
P.O. Box 2078, MS-402
Carlsbad, NM 88221-2078
123. Jeff Williams
U.S. DOE, EM-351
Trevion II Building
Washington D.C. 20585-0002
124. Peter Zombori
KFKI -Health Physics Dept.
P.O. Box 49
H-1525 Budapest Hungary
125. Office of Assistant Manager for Energy
Research and Development
Oak Ridge Operations Office
Department of Energy
P.O. Box 2008
Oak Ridge, TN 37831-6269
- 126.-127 Office of Scientific and Technical Infor.
P.O. Box 62
Oak Ridge, TN 37831